INTERNATIONAL JOURNAL OF HYDROGEN ENERGY 43 (2018) 8936–8943

Available online at www.sciencedirect.com

ScienceDirect

journal homepage: www.elsevier.com/locate/he

Dynamics and spatial distribution of water in Nafion 117 membrane investigated by NMR spin-spin relaxation

Heber E. Andrada [a,b], *María B. Franzoni* [a,b], *Alejo C. Carreras* [a,b,**], *Fabián Vaca Chávez* [a,b,*]

[a] *Instituto de Física Enrique Gaviola (IFEG), CONICET, Medina Allende s/n, Ciudad Universitaria, X5016LAE Córdoba, Argentina*

[b] *Facultad de Matemática, Astronomía, Física y Computación (FaMAF), Universidad Nacional de Córdoba (UNC). Medina Allende s/n, Ciudad Universitaria, X5016LAE Córdoba, Argentina*

ARTICLE INFO

Article history:
Received 24 December 2017
Received in revised form
6 March 2018
Accepted 16 March 2018
Available online 12 April 2018

Keywords:
Nafion membranes
Water dynamics
NMR
Spin–spin relaxation

ABSTRACT

The dynamics and spatial distribution of water molecules in Nafion 117 membrane has been investigated by ^{1}H NMR. To this end, 1D and 2D spin-spin (T_2) relaxometry experiments were carried out as a function of the relative humidity ranging from 9 to 100%. The inverse Laplace transform was successfully applied to obtain the 1D T_2 distributions and 2D relaxation maps. The 1D T_2 distributions show two peaks at low RH and mainly one at high water content, which can be associated with the rearrangement of the exchange sites inside the polymeric channels with the amount of water. From the T_2 distribution at 70% RH three types of water were identified corresponding to different degree of molecular mobility. The 2D T_2-T_2 maps show molecular exchange between the two water populations found at low RH, while at 70% the exchange between only the two more mobile water populations takes place.

Introduction

A fuel cell is a device that converts the chemical energy from a fuel into electricity through a chemical reaction [1]. Proton exchange membrane fuel cells (PEMFCs) are considered the most promising type of fuel cell for several applications [2,3]. A PEMFC is built out of a membrane electrode assembly (MEA) which includes two electrodes, the electrolyte membrane, the catalyst, and two gas diffusion layers [4].

The electrolyte membrane is a key component in a PEM fuel cell. An optimal membrane for use in PEM fuel cells must have a high proton conductivity, low electron conductivity, low fuel permeability, good chemical and thermal stabilities, and good mechanical properties [5]. One of the most common and commercially available fuel cell electrolytes is the Nafion® membrane, manufactured by DuPont. Nafion is a copolymer of tetrafluoroethylene and a vinyl ether containing a sulfonyl fluoride group at the end. Fig. 1 shows the Nafion chemical structure and a scheme of the cluster-channel or cluster-

* *Corresponding author*. Instituto de Física Enrique Gaviola (IFEG), CONICET. Medina Allende s/n, Ciudad Universitaria, X5016LAE, Córdoba, Argentina.
** *Corresponding author* Instituto de Física Enrique Gaviola (IFEG), CONICET. Medina Allende s/n, Ciudad Universitaria, X5016LAE, Córdoba, Argentina.
E-mail addresses: acarreras@famaf.unc.edu.ar (A.C. Carreras), fvacachavez@famaf.unc.edu.ar (F.V. Chávez).
https://doi.org/10.1016/j.ijhydene.2018.03.124
0360-3199/

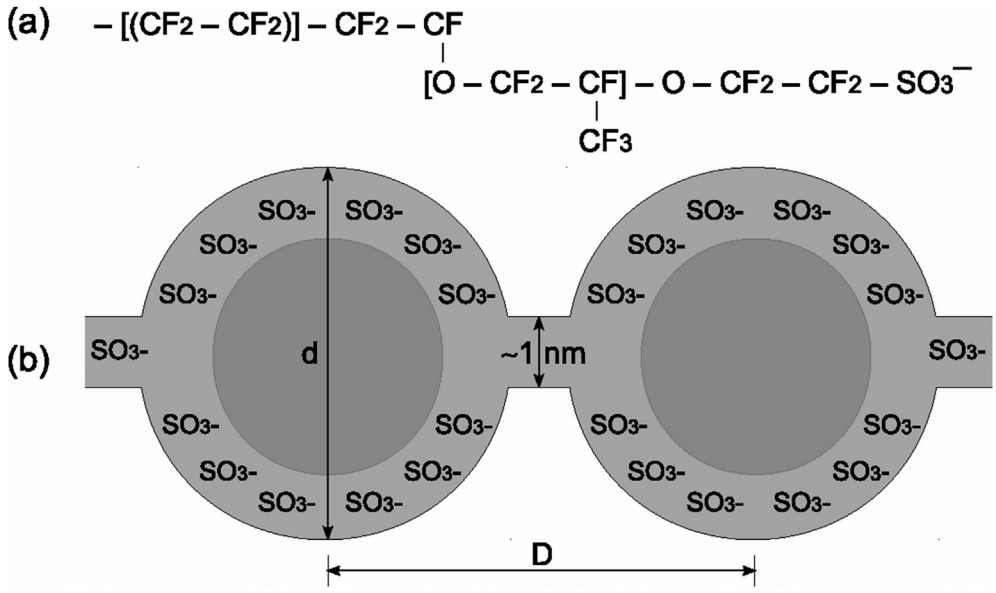

Fig. 1 – (a) Chemical structure and (b) channel morphology of Nafion according to the cluster-channel model where *d* is the cluster diameter and *D* is inter-cluster distance (see text) [6–9].

network model where *d* is the cluster diameter and *D* is inter-cluster distance, which depend on the water content (*vide infra*) [6–9].

The water balance is a critical issue in the performance and lifetime of PEM fuel cells. The efficiency of a PEMFC depends on the proton conductivity of the electrolyte membrane, and in turn, the proton conductivity of a Nafion membrane strongly depends on the water content of the polymer [10,11]. Therefore, it is very important to have a good knowledge of the water dynamics and the spatial distribution of water molecules within the polymer channels.

In this sense, the Nuclear Magnetic Resonance (NMR) is a well-established technique useful for studying the molecular dynamics in a wide range of systems. Proton nuclear magnetic relaxation (^{1}H NMR) has been successfully used for the study of molecular dynamics of confined systems such as liquid crystals in random porous glass [12], water in porous polymeric networks [13,14] and modified Nafion membranes incorporating cations of ionic liquids [15,16]. The nuclear spin relaxation times of confined systems in porous media are determined by the chemical and physical environments. Consequently, measurements of spin-lattice (T_1) and spin-spin (T_2) relaxation times provide information on molecular dynamics, pore size, tortuosity and liquid-surface interactions. In the case of electrolyte membranes they are related to interactions between chemical species within the proton conductive channels. When two or more liquid populations can be identified, for instance two different pore sizes within the porous media, 2D NMR gain importance. These experiments consists on three main parts, an initial encoding block is followed by a mixing time and finally a detection block is applied. The encoding and detection blocks are set in such a way that either longitudinal T_1 and/or transverse T_2 relaxation are involved and correlation functions such as T_1-T_1; T_1-T_2; T_2-T_2 are measured [17]. The mixing time between encoding and detection allows diffusive exchange among different spin populations. The inversion of the 2D data through a numerical Laplace inversion (NLI) algorithm [18] generates a 2D relaxation map. While diagonal peaks reflect the number of molecules present in each environment, off-diagonal peaks in the map are related to the exchange process.

There are several theoretical and experimental studies related with the dynamics of water in Nafion membranes. Raso et al. reported a mathematical model to describe the diffusivity of water in Nafion 117 membranes and the relationship between the water content in the membrane and the water activity [19]. Urata et al. [20] studied the static and dynamic properties of the water in swollen perfluorinated membranes by molecular dynamics simulations and they reported three groups of water according to different molecular interactions.

On the other hand, Kunimatsu et al. [21] characterized the water distribution in hydrated Nafion membranes using Attenuated Total Reflectance Fourier Transform Infrared Spectroscopy. Xu et al. studied the water dynamics by ^{1}H T_1 NMR relaxometry through the Fast Field Cycling technique [22] and they analysed the T_1 profiles using the well known Bloembergen, Pourcell and Pound (BPP) model [23]. Kim et al. [24] performed a multi-exponential fit of the ^{1}H transversal magnetization decay of water proton. Nicotera et al. investigated the dynamics of water molecules in Nafion membranes with and without the addition of sulfated titania nanoparticles by NMR spectroscopy and pulsed field gradient diffusion [25]. In these contributions, the authors reported two types of water corresponding to molecules with different mobility.

In this work, the spatial distribution of water molecules within the proton conductive channels of Nafion 117 membrane was studied as a function of water content. To this end, the ^{1}H NMR spin-spin relaxation time (T_2) was measured at several relative humidities (RH) from 9% to 100%. In addition, two-dimensional (2D) T_2-T_2 exchange experiments were also

performed to study the molecular exchange between water populations.

Experimental

Sample preparation

A commercial Nafion 117 polymeric membrane (Dupont) was chosen for the present study. Prior the NMR measurements, the Nafion membrane samples were subjected to a pretreatment in order to increase the water uptake (see, for instance Ref. [26]). The pretreatment consisted on:

- heating in Milli-Q water up to 80 °C, and keep this temperature for 1 h;
- rinsing with Milli-Q water;
- heating in hydrogen peroxide 3% solution up to 80 °C, and keep this temperature for 1 h;
- rinsing with Milli-Q water;
- heating in a 0.5 M H_2SO_4 solution up to 80 °C, and keep this temperature for 1 h;
- rinsing with Milli-Q water;
- keep under water.

In order to obtain the desired water content in the samples, membrane strips were placed at the bottom of a standard 5 mm NMR tube. A porous separator was set above the membrane strips and a small tube (2.5 mm OD) containing a saturated solution of the corresponding salt was inserted to control the humidity within the NMR tube, as shown in Fig. 2a. Then, the tubes were sealed and allowed to equilibrate over a minimum period of 1 month. Greenspan [27] reported temperature dependence, between 0 and 100 °C, of the equilibrium relative humidities of saturated salt solutions in the range of 3–98%. Fig. 2b presents the list of the salts used in this work and the corresponding relative humidities. The 100% RH corresponds to a fully hydrated membrane which was obtained by direct contact with distilled water.

NMR measurements

Measurements were carried out in a 1.4 T spectrometer, operating at 60 MHz for protons, equipped with a permanent magnet (Varian EM 360) and a Magritek Kea2 console. For the proton spin-spin relaxation time, T_2, the Carr-Purcell-Meiboom-Gill (CPMG) [28] sequence was employed. The length of the $\pi/2$ radiofrequency pulse was set to 16 μs, the echo time was $\tau = 100$ μs and the number of echoes was varied between 500 and 1000. The data were processed by means of a 1D numerical Laplace inversion to obtain the T_2 distributions [18].

The T_2-T_2 pulse sequence consists of two CPMG sequences connected by a mixing period, t_m, as is schematized in Fig. 3a. The first CPMG block gives the indirect dimension of the 2D experiment and the magnetization evolves a time $\tau_1 = M\tau$, where M is increased every new experiment. During this first encoding period, the T_2 value labels each initial spin population in each given chemical environment. During t_m the magnetization is stored in the z direction, and therefore no transverse relaxation occurs but molecules could migrate to a different chemical environment during this period. After t_m a

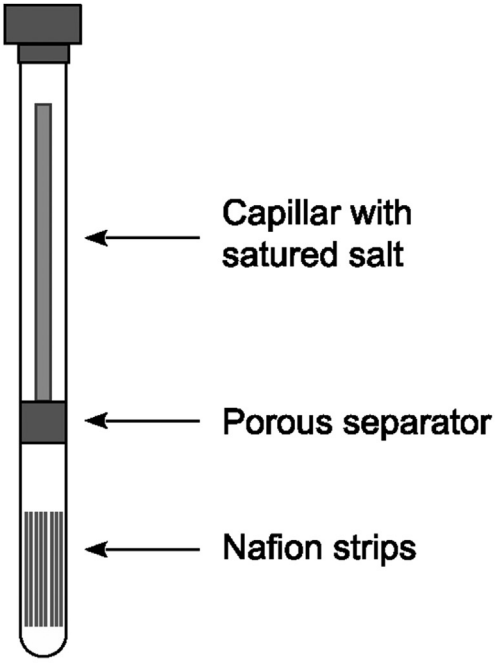

(a)

Salt	RH (%)
KOH	9
KAc	23
K2CO3	43
KI	70
(NH4)2SO4	81
H2O	100

(b)

Fig. 2 – (a) Sketch of a sample as prepared for NMR analysis. (b) Table with the salts used and the corresponding relative humidities according to Ref. [27].

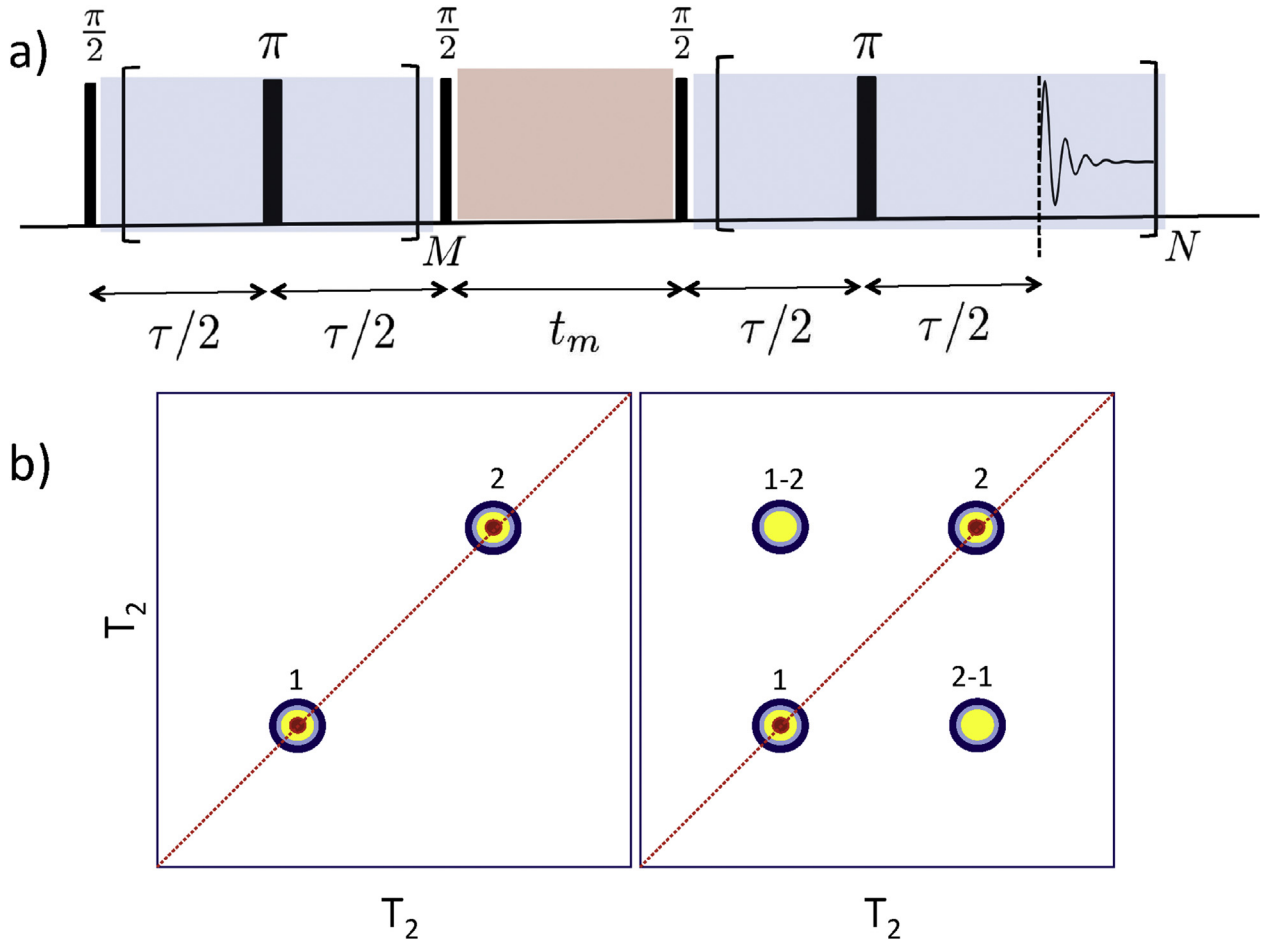

Fig. 3 – a) Pulse sequence used for 2D $T_{-2}T_2$ correlation experiments. The experimental values for τ and t_m are described in the text. b) Scheme of the 2D relaxation maps for the case of two spin populations with different spin-spin relaxation times without (left panel) and with (right panel) molecular exchange.

second CPMG sequence is applied and the magnetization evolves a time $\tau_2 = N\tau$ where N is the dimensionality of the direct dimension which represents the number of acquired points. If there is molecular exchange during the mixing period, the T_2 labeling of the second block will differ from the one of first block. After M experiments with N acquisitions, a $M \times N$ data matrix is collected. By performing a numerical Laplace inversion of the resulting 2D data a 2D T_2-T_2 map is generated and here the algorithm proposed by Teal and Eccles [29] was used which is based on the fast iterative shrinkage-thresholding algorithm (FISTA) (see Ref. [30] for a comparison of different approaches for the numerical Laplace inversion of the 2D data). As an example, in Fig. 3b the relaxation maps for the case of two spin populations, **1** and **2**, with different spin-spin relaxation times are schematized. When no molecular exchange occurs during the mixing time, the relaxation map shows two peaks on the diagonal, corresponding to both relaxation rates. Peaks on the off-diagonal part of the 2D matrix indicate the molecular exchange from one population to the other. For the experiments, 1000 echoes with echo time of $\tau = 100$ μs were acquired in the direct dimension while 32 logarithmically spaced points were used for the indirect dimension.

Results and discussion

Fig. 4 presents the T_2 distribution profiles for water in Nafion 117 membrane at different relative humidities increasing from 9 to 100%.

The results reveal two different scenarios: for RH below and above 70%. While at low water content the distributions present clearly two T_2, at higher humidities mainly one is found. The two characteristic T_2 values can be assigned to two different water populations. On the one hand, the population with the shortest T_2 value corresponds to water molecules with less mobility, and can be interpreted as the molecules that are bounded to the sulfonic groups of the polymer chains. On the other hand, the molecules with higher T_2 value have greater mobility, and are located far from the sulphonic groups. As the amount of water increases from 9 to 43% the two populations persist but the T_2 values increase, indicating a higher water mobility. At 70% RH the T_2 distribution presents three peaks corresponding to three different types of water, which is in agreement with the results reported by Devanathan et al. [31] and Urata et al. [20] obtained through molecular dynamics simulation. The authors distinguish three types of

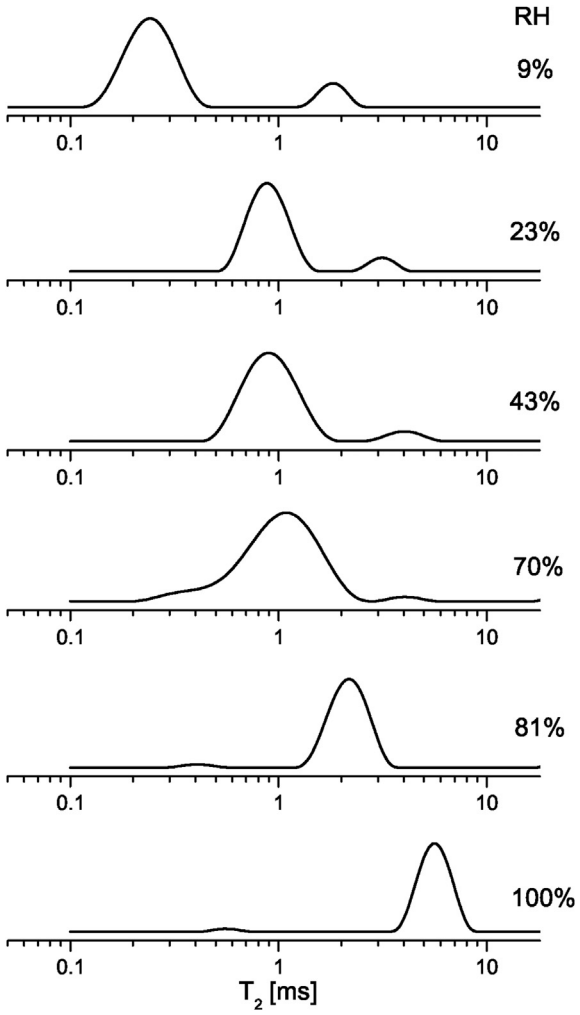

Fig. 4 – Water proton T_2 distribution profiles in Nafion 117 membrane at different relative humidities, increasing from 9 to 100%.

water regarding the interaction with the sulfonic groups and/or other water molecules. In the case of 81 and 100% RH the T_2 distributions also show two peaks but most of the NMR signal arises from a large reservoir of free water which eclipses the other contribution. It seems that the water dynamics is governed by those molecules with higher mobility. This finding is in agreement with Devananthan et al. (see Fig. 13 in Ref. [31]) where the authors report three types of waters at ~70% RH but at higher water content only the bound and free water domains are observed.

Similarly, in the present study the water molecules can be classified as follow:

i) *bound:* water molecules strongly interacting with the sulfonic groups.
ii) *weakly bound:* water molecules which are relatively loosely bound to the sulfonic groups.
iii) *free:* highly mobile water molecules.

An schematic of the proposed water distribution is presented in Fig. 5.

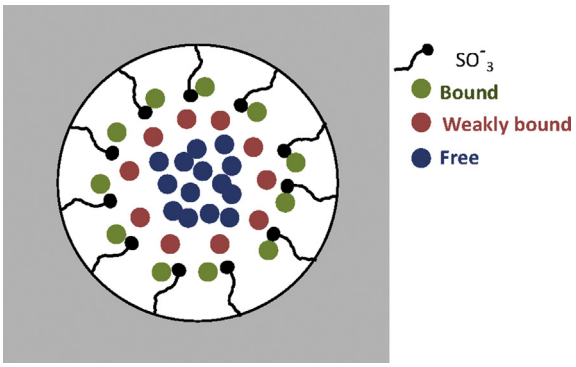

Fig. 5 – Schematic for the water distribution within the polymeric clusters.

Xu et al. [22] found evidence of two types of water, by fitting the Larmor frequency dependence of the water proton T_1 of Nafion hydrated with H_2O and D_2O. In the case of Nafion membranes hydrated with D_2O, the ^1H signal comes from the HDO residues.

Kim et al. performed a multi-exponential fit of the transversal magnetization decay of water proton, measured with the CPMG sequence, of hydrated Nafion membrane and they reported three types of water associated to different mobilities [24].

Besides the NMR results reported in the literature, Kunimatsu et al. [21] characterized the water distribution in hydrated Nafion membranes using Attenuated Total Reflectance Fourier Transform Infrared Spectroscopy (ATR-FTIR). As a function of the hydration level the authors distinguished different types of water from the δ(HOH) band of water in the spectrum: a band at 1740 cm^{-1} is associated with hydrated protons and the authors assign the band at 1630 cm^{-1} to water molecules with different degrees of hydrogen bonding between sulfonate groups and other water molecules. In the present work, using the numerical Laplace inversion, it was possible to observe from the T_2 distribution not only the different types of waters but also different features above and below 70% RH.

The water uptake, λ, follows a similar behaviour as a function of the RH: the slope of λ *vs.* RH changes to higher values above 70–80% RH, as it is well documented in the literature (see, for instance, Ref. [32] and references therein). During the hydration process, the first water molecules bind to the sulfonic groups forming a stable hydration shell (*bound water*). After this bound-water regime, up to RH ~ 70%, additional water molecules form multiple solvation shells (*bound + weakly bound water*). At higher RHs (>70%), additional water molecules lead an increase of the connectivity of the hydrophilic domains and possess higher mobility (*free water*).

A similar "crossover" reflected on the water dynamics was observed by Perrin et al. [33]. The ^1H NMR spin-lattice relaxation time, T_1, of water confined in Nafion measured at a Larmor frequency of 300 kHz increases with the water content up to a RH around 75%, then T_1 decreases. This behaviour is in agreement with Gierke et al. who proposed that upon dehydration a reorganization of exchange sites occurs, which is reflected on the cluster diameter (see Fig. 1) [6]. In order to

check that, the cluster diameter as a function of the relative humidity was calculated from data taken from the literature as follows:

From values of cluster diameter, d, and fractional weight gain m_{H_2O}/m_{dry} reported by Gierke et al. (see Table III in Ref. [6]), a linear fit was performed, obtaining:

$$d(\text{nm}) = 0.11271 \times \left(\frac{m_{H_2O}}{m_{dry}} \times 100\right) + 1.9117 \quad (1)$$

where d(nm) is the cluster diameter in nm, $m_{H_2O}(= m_{wet} - m_{dry})$ is the mass of water absorbed, and m_{wet} and m_{dry} is the mass of the wet and dry polymer, respectively.

The fractional weight gain was written as (see for example Ref. [34]):

$$\frac{m_{H_2O}}{m_{dry}} = \lambda \frac{M_{H_2O}}{EW} \quad (2)$$

where λ is the water uptake, $M_{H_2O} = 18 g mol^{-1}$ is the molecular weight of water, and $EW = 1100\ g\ mol^{-1}$ is the Nafion equivalent weight.

The relationship between λ and the relative humidity RH was taken from the analytical expression proposed by Ochi et al. [35].

$$\lambda = \sum_{n=0}^{5} a_n (RH)^n \quad (3)$$

with a_n as defined in Ref. [35].

Thus, from Eqs. (1)–(3), the cluster diameter d was calculated as a function of the relative humidity RH, and plotted in Fig. 6. The black circles correspond to the values of RH used in this work (shown in Fig. 2). The inset of Fig. 6 shows the average distance between water oxygen and its nearest sulfur (d_{O_w-S}) as a function of RH, determined from results of the simulations performed by Devanathan et al. [31]. This result also reflects the two hydration regimes (above and below 70–80% RH).

As discussed previously by Gierke et al. the cluster size depends linearly on m_{H_2O}/m_{dry} [6] (see Eq. (1)). As it can be observed in Fig. 6 the cluster size follows a quite linear dependence up to RH~70–80% and then it grows more abruptly. The growth of the cluster is attributed to an expansion and reorganization of the exchange sites.

Fig. 7 show the 2D $T-2T_2$ maps for all humidities corresponding to a mixing time $t_m = 4$ ms. Two diagonal peaks are identified at 9, 23 and 43% RH. These peaks correspond to two different water populations with two different relaxation times T_2, assigned to bound and weakly bound water. This is in agreement with the 1D data presented in Fig. 4. The water exchange among these two populations is evidenced by the presence of off-diagonal peaks that correlate the diagonal ones. At 70% RH, a third water population becomes evident since three diagonal peaks are observed. The presence of off-diagonal peaks connecting mainly the second and third diagonal peaks reveal the molecular exchange between the populations of *weakly bound* and *free* water molecules. At 81 and 100% RH only one bright peak is observed, in these cases most of the NMR signal arises from a large reservoir of water which eclipses the other contributions; for these filling levels one kind of water domains the water distributions inside the pores.

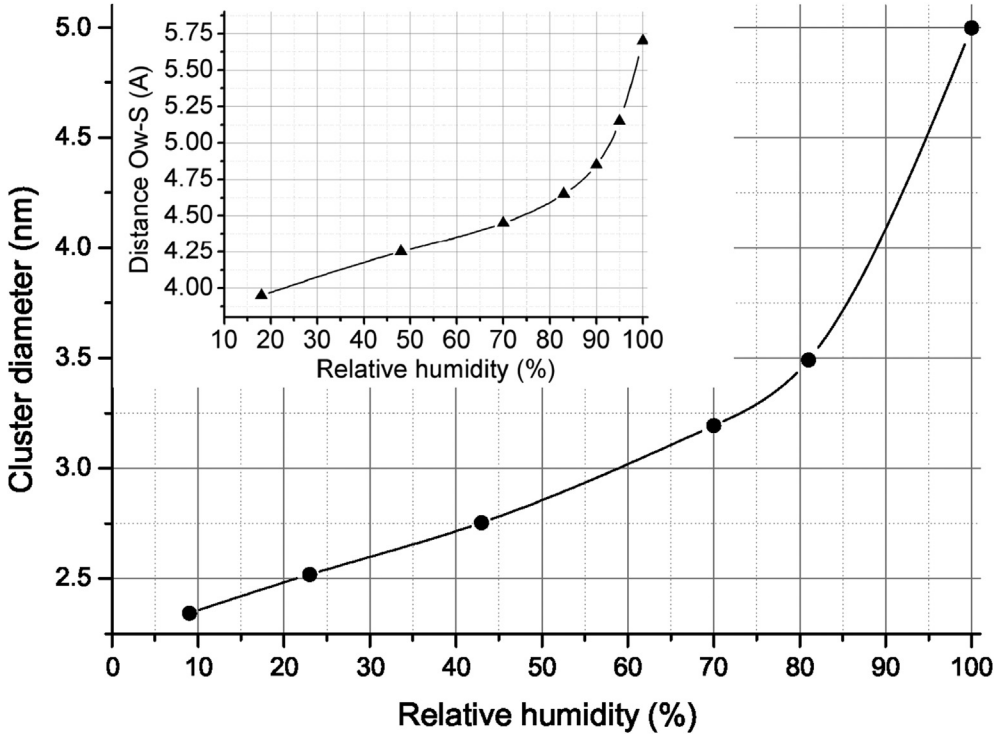

Fig. 6 – Cluster diameter as a function of relative humidity, calculated according to Gierke et al. [6], using λ values from Ochi et al. [35]. Inset: Average distance between water oxygen and its nearest sulfur, calculated from data reported by Devanathan et al. [31]. See text for details.

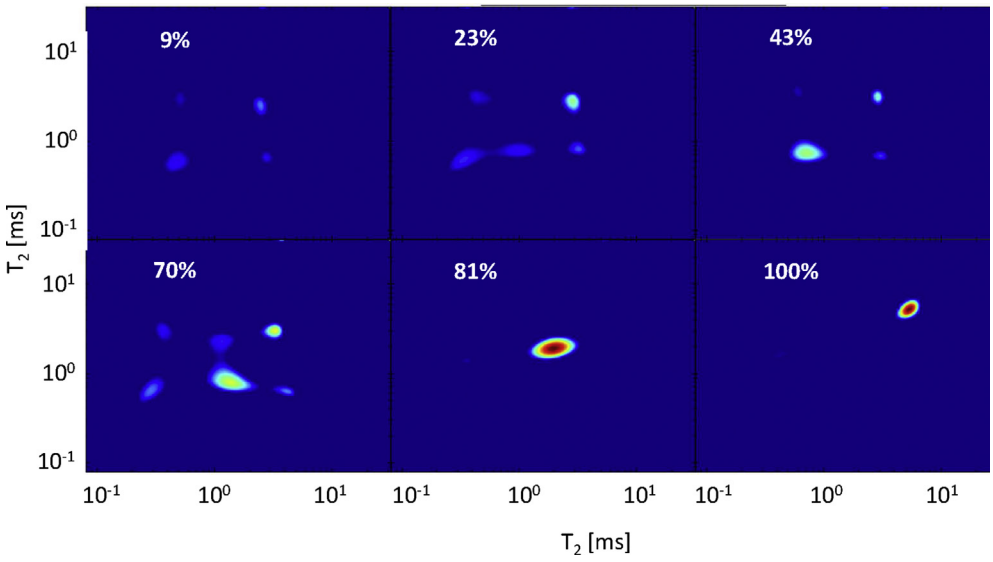

Fig. 7 – 2D T_2-T_2 exchange plots for all relative humidities corresponding to a mixing time $t_m = 4$ ms.

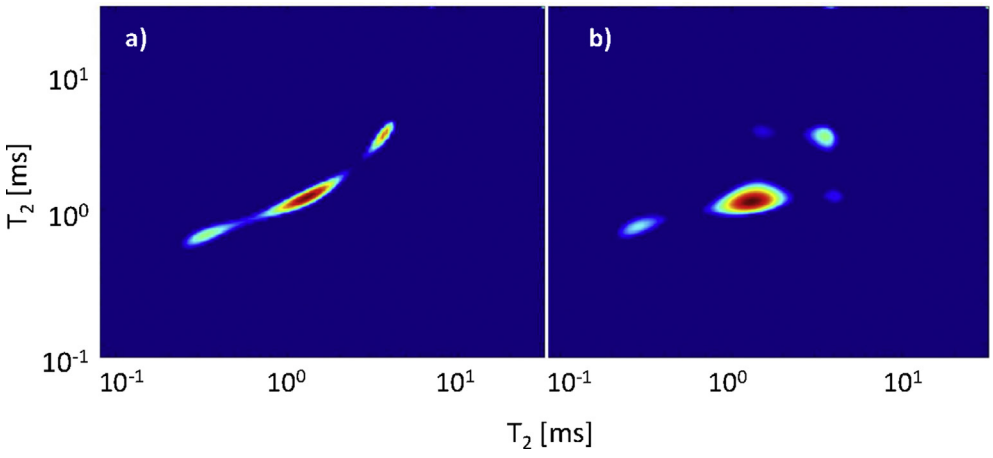

Fig. 8 – : 2D T_2-T_2 exchange plots for 70% RH at mixing times: a) $t_m = 600$ μs and b) $t_m = 1$ ms.

In order to explore the possibility of molecular exchange between the *bound* and *weakly bound* populations in the sample 70% RH additional measurements were performed at other mixing times. Fig. 8 presents the T_2-T_2 maps corresponding to $t_m = 600$ μs and $t_m = 1$ ms. For $t_m = 600$ μs no exchange is detected even between populations with the more mobile water molecules. In the case of $t_m = 1$ ms the non diagonal peaks, correlating the *weakly bound* and *free* water, evidence that the exchange dynamics among these two populations is more efficient.

Conclusions

In this work the distribution of water molecules in Nafion 117 membranes was studied as a function of the relative humidity using 1D and 2D NMR T_2 relaxometry. The 1D T_2 distributions and 2D relaxation maps were obtained by using a numerical Laplace inverse algorithm. From the 1D results, the T_2 distributions show two different features: while two peaks are present at low RH, mainly one appears at high water content. This behaviour can be correlated with the rearrangement of the exchange sites with the amount of water, which occurs at around 70–80% RH. An interesting result was obtained here in this humidity range: from the T_2 distribution at 70% RH three types of water were identified.

From the 2D T_2-T_2 maps it was possible to observe a molecular exchange between the two water populations found at low RH while at 70% the exchange between only the two more mobile water populations dominates.

Up to our knowledge, this is the first time where the inverse Laplace transform was applied to describe the dynamics and spatial distribution of water molecules in Nafion membranes. This algorithm resulted a very useful tool to process the spin relaxation 1D and 2D NMR data and can be successfully applied and extended to characterize other systems involving confined molecules in polymeric matrices.

Acknowledgements

The authors acknowledge Universidad Nacional de Córdoba (UNC), Consejo Nacional de Investigaciones Científicas y Técnicas (CONICET) and Agencia Nacional de Promoción Científica y Tecnológica (ANPCYT) from Argentina for financial support.

REFERENCES

[1] Carrette L, Friedrich KA, Stimming U. Fuel cells - fundamentals and applications. Fuel Cell 2001;1(1):5–39.
[2] Wang Y, Chen KS, Mishler J, Cho SC, Cordobes Adroher X. A review of polymer electrolyte membrane fuel cells: technology, applications, and needs on fundamental research. Appl Energy 2011;88:981–1007.
[3] Mehta V, Cooper JS. Review and analysis of pem fuel cell design and manufacturing. J Power Sources 2003;114(1):32–53.
[4] Barbir F. PEM fuel cells. Theory and practice. USA: Elsevier; 2013.
[5] de Bruijn FA, Dam VAT, Janssen GJM. Review: durability and degradation issues of PEM fuel cell components. Fuel Cell 2008;8(1):3–22.
[6] Gierke TD, Munn GE, Wilson FC. The morphology in Nafion perfluorinated membrane products, as determined by wide- and small-angle X-ray studies. J Polym Sci Polym Phys Ed 1981;19(11):1687–704.
[7] Hsu WY, Gierke TD. Ion transport and clustering in Nafion perfluorinated membranes. J Membr Sci 1983;13(3):307–26.
[8] Heitner-Wirguin C. Recent advances in perfluorinated ionomer membranes: structure, properties and applications. J Membr Sci 1996;120(1):1–33.
[9] Mauritz KA, Moore RB. State of understanding of Nafion. Chem Rev 2004;104(10):4535–85.
[10] Schmittinger W, Vahidi A. A review of the main parameters influencing long-term performance and durability of PEM fuel cells. J Power Soures 2008;180(1):1–14.
[11] Dai W, Wang H, Yuan X-Z, Martin JJ, Yang D, Qiao J, et al. A review on water balance in the membrane electrode assembly of proton exchange membrane fuel cells. Int J Hydrogen Energy 2009;34(23):9461–78.
[12] Vilfan M, Apih T, Sebastião PJ, Lahajnar G, Žumer S. Liquid crystal 8CB in random porous glass: NMR relaxometry study of molecular diffusion and director fluctuations. Phys Rev E 2007;76(5):051708.
[13] Silletta EV, Velasco MI, Gómez CG, Acosta RH, Strumia MC, Monti GA. Evaporation kinetics in swollen porous polymeric networks. Langmuir 2014;30(14):4129–36.
[14] Silletta EV, Velasco MI, Gomez CG, Strumia MC, Stapf S, Mattea C, et al. Enhanced surface interaction of water confined in hierarchical porous polymers induced by hydrogen bonding. Langmuir 2016;32(29):7427–34.
[15] Martins CF, Neves L, Coelhoso IM, Vaca Chávez F, Crespo JG, Sebastião PJ. Temperature effects on the molecular dynamics of modified Nafion membranes incorporating ionic liquids' cations: a ^{1}H NMRD study. Fuel Cell 2013;13(6):1166–76.
[16] Neves LA, Sebastião PJ, Coelhoso IM, Crespo JG. Proton NMR relaxometry study of Nafion membranes modified with ionic liquid cations. J Phys Chem B 2011;115(27):8713–23.
[17] Song Y-Q. Magnetic resonance of porous media (MRPM): a perspective,. J Magn Reson 2013;229:12–24.
[18] Venkataramanan L, Song Y-Q, Hurlimann MD. Solving Fredholm integrals of the first kind with tensor product structure in 2 and 2.5 dimensions. IEEE Trans Signal Process 2002;50(5):1017–26.
[19] Raso M, Leo T, González-Espasandín O, Navarro E. New expressions to determine the water diffusion coefficient in the membrane of PEM fuel cells. Int J Hydrogen Energy 2016;41(43):19766–70.
[20] Urata S, Irisawa J, Takada A, Shinoda W, Tsuzuki S, Mikami M. Molecular dynamics simulation of swollen membrane of perfluorinated ionomer. J Phys Chem B 2005;109(9):4269–78.
[21] Kunimatsu K, Bae B, Miyatake K, Uchida H, Watanabe M. ATR-FTIR study of water in Nafion membrane combined with proton conductivity measurements during hydration/dehydration cycle. J Phys Chem B 2011;115(15):4315–21.
[22] Xu F, Leclerc S, Canet D. NMR relaxometry study of the interaction of water with a Nafion membrane under acid, sodium, and potassium forms. evidence of two types of bound water. J Phys Chem B 2013;117(21):6534–40.
[23] Bloembergen N, Purcell EM, Pound RV. Relaxation effects in nuclear magnetic resonance absorption. Phys Rev 1948;73(7):679–712. https://doi.org/10.1103/PhysRev.73.679.
[24] Kim YS, Dong L, Hickner MA, Glass TE, Webb V, McGrath JE. State of water in disulfonated poly(arylene ether sulfone) copolymers and a perfluorosulfonic acid copolymer (Nafion) and its effect on physical and electrochemical properties. Macromolecules 2003;36(17):6281–5.
[25] Nicotera I, Simari C, Boutsika LG, Coppola L, Spyrou K, Enotiadis A. NMR investigation on nanocomposite membranes based on organosilica layered materials bearing different functional groups for PEMFCs. Int J Hydrogen Energy 2017;42(46):27940–9.
[26] Kuwertz R, Kirstein C, Turek T, Kunz U. Influence of acid pretreatment on ionic conductivity of Nafion membranes. J Membr Sci 2016;500(Suppl. C):225–35.
[27] Greenspan L. Humidity fixed points of binary saturated aqueous solutions. J Res NBS A Phys Ch 1977;81A(1):89–96.
[28] Meiboom S, Gill D. Modified spin-echo method for measuring nuclear relaxation times. Rev Sci Instrum 1958;29(8):688–91.
[29] Teal PD, Eccles C. Adaptive truncation of matrix decompositions and efficient estimation of NMR relaxation distributions. Inverse Probl 2015;31(4):045010.
[30] Silletta EV, Franzoni MB, Monti GA, Acosta RH. Probing numerical Laplace inversion methods for two and three-site molecular exchange between interconnected pore structures. J Magn Reson 2018;286:82–90.
[31] Devanathan R, Venkatnathan A, Dupuis M. Atomistic simulation of Nafion membrane i. effect of hydration on membrane nanostructure. J Phys Chem B 2007;111(28):8069–79.
[32] Kusoglu A, Weber AZ. New insights into perfluorinated sulfonic-acid ionomers. Chem Rev 2017;117(3):987–1104.
[33] Perrin J-C, Lyonnard S, Guillermo A, Levitz P. Water dynamics in ionomer membranes by field-cycling nmr relaxometry. Fuel Cell 2006;6(1):5–9.
[34] Xu F, Leclerc S, Lottin O, Canet D. Impact of chemical treatments on the behavior of water in Nafion nre-212 by 1h nmr: self-diffusion measurements and proton quantization. J Membr Sci 2011;371(1):148–54.
[35] Ochi S, Kamishima O, Mizusaki J, Kawamura J. Investigation of proton diffusion in nafion117 membrane by electrical conductivity and NMR. Solid State Ionics 2009;180:580–4.